AAPS PharmSciTech, Vol. 10, No. 1, March 2009 (© 2009)
DOI: 10.1208/s12249-009-9193-6

Research Article

Physicochemical Characteristics, Cytotoxicity, and Antioxidant Activity of Three Lipid Nanoparticulate Formulations of Alpha-lipoic Acid

Uracha Ruktanonchai,[1,6] Piyawan Bejrapha,[1] Usawadee Sakulkhu,[1] Praneet Opanasopit,[2] Nuntavan Bunyapraphatsara,[3,4,5] Varaporn Junyaprasert,[3,4,5] and Satit Puttipipatkhachorn[3,4,5]

Received 5 September 2008; accepted 31 December 2008; published online 12 March 2009

Abstract. Exogenously supplied alpha-lipoic acid (LA) has proven to be effective as an antioxidant. In an effort to develop a water-soluble formulation for topical administration, LA was formulated in the form of solid lipid nanoparticles (SLN), nanostructure lipid carriers (NLC), and nanoemulsion (NE) and characterized in terms of physical and biological properties. Mean particle size of 113, 110, and 121 nm were obtained for NE, NLC, and SLN, respectively, with narrow size distribution. Zeta potential was approximately in the range of −25 to −40 mV. Disc and spherical structures of nanoparticles were observed by cryo-scanning electron microscopy. Entrapment efficiency of LA in three formulations was found to be more than 70%. After 120 days of storage at 25°C, physical stability of all formulations remained unchanged whereas the entrapment efficiency of SLN and NLC could be maintained, suggesting relative long-term stability. Prolonged release of LA formulation following the Higuchi model was found where a faster release was observed from NE compared with that of SLN and NLC. More than 80% of cell survivals were found up to 1 μM of LA concentrations. Antioxidant activity analysis demonstrated that all LA-loaded formulations expressed antioxidant activity at a similar magnitude as pure LA. These results suggest that chosen compositions of lipid nanoparticles play an important role on drug loading, stability, and biological activity of nanoparticles. Both SLN and NLC demonstrated their potential as alternative carriers for aqueous topical administration of LA.

KEY WORDS: alpha-lipoic acid; antioxidation activity; nanoemulsion; nanostructure lipid carriers; solid lipid nanoparticles.

INTRODUCTION

More recently, alpha-lipoic acid (LA) and its reduced form (dihydrolipoic acid; DHLA) are well-known as potent antioxidants both *in vitro* and *in vivo*. Exogenously supplied LA and DHLA are effective at preventing or lessening damage caused by reactive oxygen species (1–7). Therefore, both LA and DHLA have been suggested for prevention and treatment of oxygen-related diseases (8,9) as well as improving diabetic peripheral, cardiac autonomic neuropathy, and cardiovascular disease (10,11). However, systemic delivery of antioxidants to the target site is still inefficient; topical application could be beneficial if sufficient quantities of the substance penetrate the skin. According to Fuchs and Milbradt, both intracutaneously injected DHLA and orally administered LA are effective in skin protection against inflammation (12). Therefore, topical application of exogenous LA could be one of the possible approaches to enhance antioxidation defense in human (13,14). Despite its most promising properties, problems related to their poor water solubility and strong sulfur smell of LA have to be resolved before they are used as an alternative supplement.

Solid lipid nanoparticles (SLN) are colloidal carriers developed at the beginning of the 1990s by RH Müller (15–17), as an alternative system to the existing traditional carriers (emulsions, liposomes, and polymeric nanoparticles), especially for the delivery of poorly water-soluble compounds both for pharmaceutical (18) and cosmetic ingredients (19,20). This is due to the vast advantages of these SLN such as the use of biocompatible and physiological lipids, avoidance of organic solvents in the preparation process, high bioavailability, controlled release rates, and suitability to large-scale production and sterilization (16,21–22). However, SLN also possesses some

[1] National Nanotechnology Center, National Science and Technology Development Agency, 111 Thailand Science Park, Paholyothin Road., Klong 1, Klong Luang, Pathumthani 12120, Thailand.
[2] Faculty of Pharmacy, Silpakorn Univerity, Nakhonpathom, Thailand.
[3] Department of Pharmacognosy, Faculty of Pharmacy, Mahidol University, Sri-ayudhya Road, Bangkok, 10400, Thailand.
[4] Department of Pharmacy, Faculty of Pharmacy, Mahidol University, Sri-ayudhya Road, Bangkok, 10400, Thailand.
[5] Department of Manufacturing Pharmacy, Faculty of Pharmacy, Mahidol University, Sri-ayudhya Road, Bangkok, 10400, Thailand.
[6] To whom correspondence should be addressed. (e-mail: uracha@nanotec.or.th)

ABBREVIATIONS: DHLA, dihydrolipoic acid; LA, alpha-lipoic acid; NE, nanoemulsion; NLC, nanostructure lipid carriers; SLN, solid lipid nanoparticles; ROS, reactive oxygen species; *Z*, ave particle diameter; MW, molecular weight; PDI, polydispersity index; ZP, zeta potential; PCS, photon correlation spectroscopy; SEM, scanning electron microscopy; TEM, transmission electron microscope; DSC, differential scanning calorimetry; ΔH, melting enthalpy; RI, recrystallization index; HPLC, high-performance liquid chromatography; EE, entrapment efficiency; FBS, fetal bovine serum; NHF, human foreskin fibroblast; DMEM, Dulbecco's modified Eagle's medium; MTT, 3-(4,5-dimethylthiazol-2-yl)-2,5-diphenyl-tetrazolium bromide; PBS, phosphate buffer saline; SD, standard deviation; *p* value, probability value.

limitations, i.e., low drug payload and possibility of drug expulsion because of change in lipid modification during storage (22). As a result, the concept of less-ordered inner structure of nanostructured lipid carriers (NLC) has been introduced. NLC can be prepared either by blending any solid and liquid lipids or by mixing special combinations of solid and liquid lipids leading to amorphous solids (23). As a result of these features, high drug payload, avoidance or minimization of drug expulsion, and enhancement of chemical stability can be achieved.

In this study, lipid nanoparticles were employed as a major carrier to increase not only drug loading but also to mimic its chemically labile properties such as chemical degradation resulting in unpleasant odor. Water-insoluble LA was prepared into three types of easy-to-use topical formulations, which are SLN, NLC, and nanoemulsion (NE). These formulations were characterized in terms of physical properties such as particle size, zeta potential, morphology, percentage of entrapment efficiency, long-term stability, crystallization behavior, and biological characteristics such as *in vitro* cytotoxicity. *In vitro* evaluation of the antioxidant activity of LA formulations was performed in human cells and compared with that of pure LA.

MATERIALS AND METHODS

Materials

The following materials were used from the indicated sources without further purification procedures. Miglyol 812® (caprylic/capric triglycerides, medium-chain triglycerides) was obtained from the Sun Chemical Co., Ltd. (Sasol, Germany). Apifil was obtained from Gattefossé, France. Alpha LA was purchased from Chemico Inter Corporation (Germany); Pluronic® F68 (Poloxamer 188) was provided as a kind sample from Vita Inc. (BASF, Germany). Methanol, acetonitrile, dichloromethane, and acetone were obtained from Fisher Scientific (UK). Acetic acid and phosphoric acid were obtained from VWR International, Ltd. (UK). Dulbecco's modified Eagle's medium (DMEM) and 3-(4,5-dimethylthiazol-2-yl)-2,5-diphenyl-tetrazolium bromide (MTT) were obtained from Sigma-Aldrich (USA). Fetal bovine serum (FBS) was purchased from Biochrom AG (Germany). L-glutamine, penicillin G sodium, streptomycin sulfate, and amphotericin B were obtained from Invitrogen Corp. (USA). Amicon® Ultra4, MW cutoffs 30 K, was obtained from Millipore, USA. Polyethersulfone ultrafiltration membrane, MW cutoff 500 K, was obtained from Millipore, USA. The water used for all experiments was purified water obtained from MilliQ Plus (Millipore, Schwalbach, Germany). All other reagents used were commercially available and were of analytical grade.

Methods

Preparation of SLN, NLC, and NE

The preparation of aqueous SLN dispersions was carried out according to the method described by Müller et al. (16). Apifil, Miglyol 812®, and Pluronic® F68 were used as solid lipid, liquid lipid, and emulsifying agent, respectively. SLN, NLC, and NE containing 1% (*w*/*w*) of LA were produced using the hot homogenization technique. The composition of each formulation is illustrated in Table I. Briefly, the melted lipid phase containing solid lipid, liquid lipid, and LA was dispersed in a hot surfactant solution of 2.5% (*w*/*w*) Pluronic® F68 (75°C), obtaining a pre-emulsion by high-speed stirring using an Ultra-Turrax T25 (6,500 rpm; IKA-Werke, Germany). This hot pre-emulsion was further processed by high-pressure homogenizer (EmulsiFlex-C3, Avestin, Canada) for three cycles at a pressure of 500 bars and 85°C. The lipid dispersion was cooled at ambient conditions to room temperature and solidified to obtain the aqueous SLN, NLC, and NE dispersions.

Particle Diameter, Zeta Potential, and Morphology Measurements

Measurement of hydrodynamic diameter, polydispersity index (PDI), and zeta potential (ZP) of the nanoparticles was performed using photon correlation spectroscopy (PCS; NanoZS4700 nanoseries, Malvern Instruments, UK). For size measurement, all the formulations were diluted with 1 mL of 0.22 μm filtered deionized water to eliminate the effect of viscosity caused by the ingredients. The zeta potential measurements were performed in distilled water which was adjusted to a conductivity of 50 μS/cm with 0.90% (*w*/*v*) sodium chloride solution. Hydrodynamic diameter, PDI, and ZP were reported as the average of three measurements at 25°C. The refractive index of SLN, NLC, NE, and water were set at 1.46, 1.46, 1.46, and 1.33, respectively. For stability studies, all samples were kept at 25°C over a period of 120 days and particle size and zeta potential measurements were undertaken every 30 days.

Cryo-Scanning Electron Microscopy

The morphology of SLN and NLC were observed by a Cryo-scanning electron microscopy (SEM; JEOL, JSM-5410LV, Japan). A drop of each sample was filled into brass rivets and plunged frozen in liquid nitrogen slush. Then, samples were then transferred into the cryo-stage of the microscope. The samples were imaged using cryo-mode at ×10,000 magnification and 15 kV.

Differential Scanning Calorimetry

To determine the degree of crystallinity of the particle dispersions, a differential scanning calorimeter (DSC; DSC823e, Mettler Toledo, Switzerland) was used. SLN and NLC were accurately weighed at 3.0–4.0 mg per aluminum pan and scanned over the range of 10°C to 80°C, with a heating rate of 10°C/min and an empty standard aluminum pan was used as reference. The melting enthalpy readings (ΔH) obtained by integration of the area under the transition thermogram peak and the recrystallization index (RI), expressed as a percentage, were calculated from the following equation (24).

$$\%\mathrm{RI} = \frac{\Delta H_{\text{aqueous SLN or NLC}}}{\Delta H_{\text{bulk material}} \times \text{concentration}_{\text{lipid phase}}(\%)} \times 100 \quad (1)$$

For stability studies, all samples were kept at 25°C over a period of 120 days and DSC measurement was undertaken every 30 days.

Table I. Composition of LA-Loaded NE, NLC, and SLN Formulations, % (*w*/*w*)

Formulations	Alpha-lipoic acid	Lipid	Surfactant (Pluronic® F68)
NE	1%	9% Miglyol 812®	2.5%
NLC	1%	8% Apifil 1% Miglyol 812®	2.5%
SLN	1%	1% Apifil	2.5%

NE nanoemulsion, *NLC* nanostructure lipid carriers, *SLN* solid lipid nanoparticles

Determination of LA Entrapment Efficiency

The entrapment efficiency (%EE) of LA in each formulation was evaluated by centrifugal filtration to separate entrapped LA. Briefly, 0.5 mL of alpha-lipoic-acid-loaded formulation was placed into centrifugal filter (Amicon® Ultra4; Millipore, USA) with molecular weight cutoffs 30 K and centrifuged at 13,000 rpm for 1.5 h at 4°C. The supernatant was removed and the sediment in the membrane was transferred into a centrifuge tube and weighed prior to extraction by addition of 4 mL of acetone and sonicated for 60 min. Quantitative analysis of LA levels in the extract was performed on 10-μL aliquots of this extract by high-performance liquid chromatography (HPLC) on a WaterE600 system with photodiode array detector equipped using Eclipse Zorbax XDB-C18 (Agilent, 250×4.6 mm, 5 μm) analytical column and Zorbax XDB-C18 (Agilent, 12.5×4.6 mm, 5 μm) guard column. The mobile phase consisted of a mixture of acetonitrile and 0.0025 M phosphoric acid (42:58% (*v*/*v*)), with a flow rate of 1.2 mL/min and detected at 220 nm with UV detector for 10 min. The %EE was calculated by applying Eq. 2.

$$\%EE = \frac{\text{Total amount of extracted LA}}{\text{Initial amount of LA loading}} \times 100 \qquad (2)$$

Determination of In Vitro Release of LA

The experiment was performed using static horizontal Franz diffusion cell to evaluate the amount of LA released from each formulation. Polyethersulfone ultrafiltration membrane at molecular weight cutoff of 500 K (Millipore, US) was used and mounted on the Franz diffusion cells. The surface area of the release membrane was 2.0 cm^2. The receptor medium was approximately 14 mL and composed of an aqueous solution of phosphate buffer saline (PBS), pH 5.5, and 20% ethanol and stirred by magnetic bar at 700 rpm to avoid different concentrations within the acceptor medium and to minimize stagnant layers. Each formulation (1 g) was loaded onto the membrane in the donor compartment. The temperature of the assay was accurately controlled at 32°C to mimic human skin. At certain time, 0.5-mL aliquots of the release medium were withdrawn using a syringe needle and the same volumes of freshly prepared receptor medium were added. The samples were analyzed by HPLC as previously described in triplicate.

Cell Cytotoxicity and Antioxidant Activity Test

Human foreskin fibroblast (NHF) cells were plated in 90 μL of DMEM, supplemented with 10% FBS, 1% L-glutamine, and 1% antibiotic and antimycotic formulation containing penicillin G sodium, streptomycin sulfate, and amphotericin B at a density of 8,000 cells per well in 96-well tissue culture polystyrene plate using NHF cells as a reference. When the cultures reached confluency (typically, 48 h after plating), all tested formulations at varying concentrations (0–10 μM) were added at 10 μL per well and 16 h post-incubation; 25 μL of MTT (5 mg/mL) was added to each well and then incubated for 4 h. Then, all media were removed and 100 μL of dimethyl sulfoxide were added. The plates were incubated for 30 min at 37°C and the absorbance was measured at 550 nm using a microplate reader (Universal Microplate Analyzer, Model AOPUS01 and AI53601, Packard BioScience, CT, USA). The percentage of cell viability was then calculated and compared with untreated cells as negative control. For antioxidant activity test, the method was modified according to the method described by Ernst et al. (25). The test was undertaken in similar manner as cell cytotoxicity test except that at 16 h post-incubation cell culture received a culture medium supplemented with 150 μM H_2O_2 solution (100 mL per well) prior to MTT addition.

Statistical Analysis

Values were expressed as mean±standard deviation (SD). Statistical significance of differences was examined using one-way analysis of variance followed by least significant difference post hoc test. A probability value (p) of less than 0.05 was considered to be statistically significant.

RESULTS AND DISCUSSION

Particle Size and Zeta Potential

Aqueous dispersion of water-insoluble LA can be obtained after being formulated as NE, NLC, and SLN. The size of these formulations was determined by PCS. The mean particle sizes of 113, 110, and 121 nm were obtained for NE, NLC, and SLN, respectively, with PDI values lower than 0.3, suggesting a narrow size distribution (Table II). No significant difference in particle size among these formulations was found (p value>0.05) although smaller particle size with narrow size distribution of NE was reported when compared with NLC and SLN systems (21,23). Zeta potential was employed as a useful tool to predict the physical stability of colloidal systems. When the absolute value of ZP is higher than 30 mV for colloidal formulation, the particles are likely to be electrochemically stable under the investigated condition (22). ZP values of −27.8, −34.8, and −39.6 nm were obtained for NE, NLC, and SLN, respectively. Only the ZP values of SLN and NLC were higher than |−30| mV, suggesting the potential of good physical stability.

After 120 days of storage at room temperature (25°C), the results indicated no significant changes in particle size values for NE, NLC, and SLN formulations, which remained in the nanosize range (less than 150 nm;

Table II. Mean Particle Diameters (*Z* ave), Polydispersity Index, and Zeta Potential (ZP) of LA-loaded NE, NLC, and SLN Formulations Determined at Day 0 of Storage (25°C)

Formulations	*Z* ave (nm)	PDI	ZP (mV)
NE	113±12	0.18±0.03	−27.8±2.6
NLC	103±9	0.20±0.02	−34.8±0.5
SLN	121±13	0.22±0.01	−39.6±2.4

PDI polydispersity index, *ZP* zeta potential, *NE* nanoemulsion, *NLC* nanostructure lipid carriers, *SLN* solid lipid nanoparticles

Fig. 1). A decrease in zeta potential was found for all formulations although significant decreases in ZP values between 0 and 120 days of storage were found for NE and NLC formulations (p value<0.05; Fig. 2). By combining results of particle size and ZP, it is clear that, although a decrease in ZP was found, good physical stability of nanoparticles could be obtained and particle aggregation during storage is not likely to occur. This could be due to electrostatic or steric repulsion between the particles.

Morphology Characterization

Cryo-SEM allowed us to obtain more information about particle size and shape by investigating the samples in frozen condition; thus, the samples are investigated close to their natural state. In this study, cryo-SEM was employed to confirm and visualize all formulations under ambient conditions (Fig. 3). Spherical and disc-like particles with a size in the nanometer range were observed for NE, NLC, and SLN formulations, which was in agreement with the size data determined by PCS. There was not much difference in particulate structure among types of formulations. These spherical shape of particles observed in this study were in contrast to the result of Jores et al. (21) who found two phase particles called "nanospoons" from SLN and NLC made from glyceryl behenate using cryo-transmission electron microscope (cryo-TEM). However, similar disc-shaped particles of SLN loaded with Softisan 154 and lecithin were also reported by cryo-TEM (26) whereas the spherical shape of SLN and NLC was seen using cryo-SEM (27) and SEM (28). Moreover, it is seen from micrographs that agglomeration of nanoparticles was observed, which could be due to the lipid nature of the carriers and the drying process during sample preparation prior to SEM analysis (23).

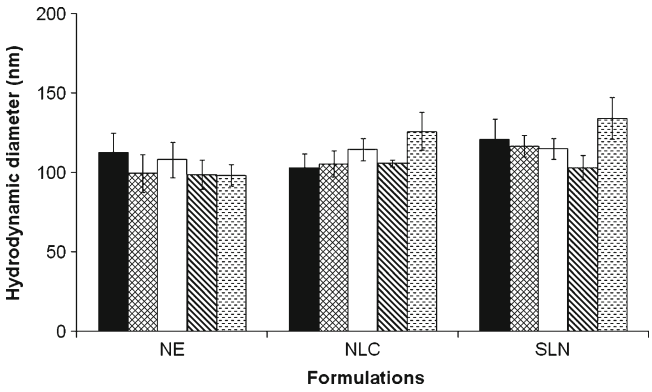

Fig. 1. Mean particle diameter (*Z* ave) of LA-loaded NE, NLC, and SLN formulations after 0 (■), 30 (▨), 60 (□), 90 (▧), and 120 (▤) days of storage at 25°C. *The mean difference is significant at the 0.05 level as compared to 0 days of storage

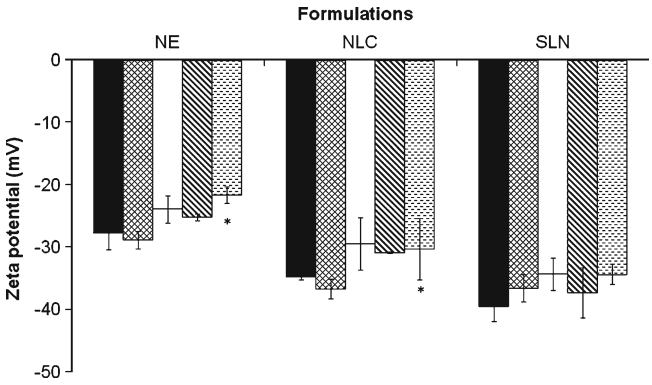

Fig. 2. Mean zeta potential of LA-loaded NE, NLC, and SLN formulations after 0 (■), 30 (▨), 60 (□), 90 (▧), and 120 (▤) days of storage at 25°C. *The mean difference is significant at the 0.05 level as compared to 0 days of storage

Differential Scanning Calorimetry

The melting and recrystallization behaviors of crystalline materials were investigated by using DSC. The recorded DSC parameters are presented in Table III. For the bulk materials, the melting process took place at 58.7°C with the maximum peak at 68.0°C and normalized enthalpy of 190.8 J/g. In case of NE, the melting behavior was not seen since LA is completely dissolved in liquid oil and no crystallization of both LA and oil can be found. For both SLN and NLC formulations, the melting peaks, including onset temperatures, were detected in the melting range of the bulk Apifil (26–78°C). Moreover, both formulations showed a significant reduction in melting temperature as compared to bulk lipid (68.0°C). This shift could be taken as an indication of the interference of SLN and NLC formation in the crystallization of Apifil, small particle size in the nanometer range, high specific surface area, and the presence of surfactants (29,30). Both enthalpy and %RI values of SLN tend to be higher compared to the NLC formulation. After production, the enthalpy and %RI of SLN and NLC tended to increase over investigation period although a higher increase rate was found in SLN formulation. A high % RI value has been used to indicate an affinity of each lipid to separate itself from formulation and become pure lipid. %RI of SLN reached 100% at 90 days (112.2%) earlier than NLC (103.7 %), which was found at 120 days, confirming delayed crystallinity properties of NLC into pure lipid over storage time. This could be due to a combination of mixed solid lipid and liquid lipid of NLC leading to a less-ordered structure of lipid matrix as well as an inhibition by dissolved LA in the melted lipid phase. This may occur during the lipid crystal growth process and allow better physical stability of LA. It has been reported that actives that are incorporated in the imperfections at the less crystalline lipid matrix of NLC provide prolonged physical stability (16,23,31).

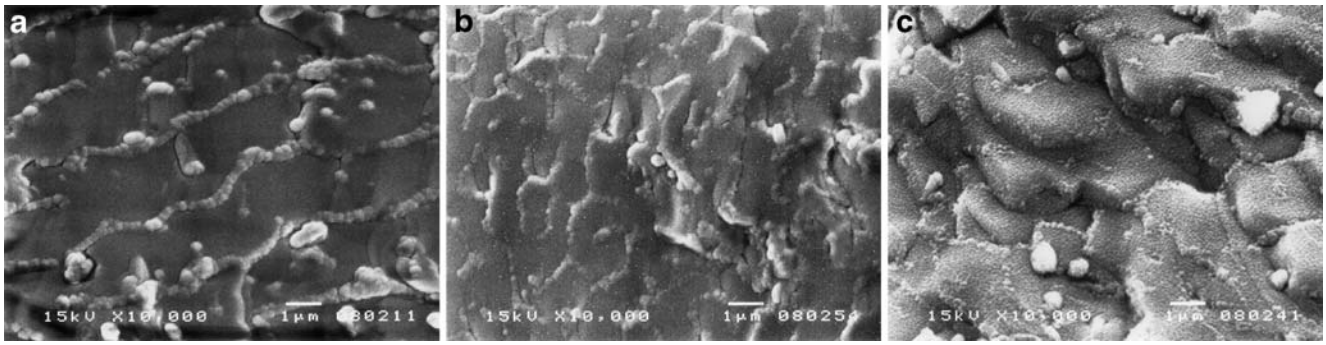

Fig. 3. Cryo-SEM micrographs of LA-loaded NE **a**, NLC **b**, and SLN **c** formulations at ×10k magnification, 15 kV

Percent Entrapment Efficiency

The formulations studied demonstrated moderate to high %EE in the range of 70–90% (*w*/*w*) observed using the centrifugation method. The experimental results demonstrated varying extent of %EE among each formulation (Fig. 4). At day 0, %EE of NE, NLC, and SLN was 80.9, 86.2, and 74.7 %, respectively. All the data of day 0 obtained from the formulations stored at 25°C were statistically compared to each other. It was found that %EE was all statistically different (p value<0.05). Therefore, the types of lipid used in formulations played an important role on %EE. NLC formulations were the most efficient to allocate LA into nanoparticles whereas SLN were the least. This finding is similar to Jenning and Gohla who found an increased stability of retinoid after loading as NLC (32,33) and Souto et al. who encapsulated clotrimazole into both SLN and NLC (34). The high %EE of NLC could be explained by the higher solubility of lipophilic compound in liquid oil than solid lipids. Moreover, for NLC systems, there was less drug expulsion due to the less-ordered inner structure of mixed solid and liquid lipid of NLC, which allow more space for the drug to be entrapped inside particle matrix (22). However, by looking at %EE *versus* storage time, an increase in storage time to 90 days of storage for NE and at 120 days of storage for NLC and SLN resulted in a significant decrease in %EE compared to those of day 0 (p value<0.05). The lowest %EE after 120 days of storage at 25°C was found to be 44.5%, 55.9%, and 55.8% for NE, NLC, and SLN, respectively. NE formulations were most inefficient at protecting LA within the nanoparticles in comparison to the other formulations. The highest %EE values were found in SLN and NLC at 120 days of storage with insignificant difference between them (p value>0.05). According to these data, NLC and SLN can be considered as more suitable carriers when compared to NE.

In Vitro Release Study: Franz Diffusion Cell

In this study, the release of LA from SLN, NLC, and NE formulation was investigated *in vitro* for 72 h **(**Fig. 5). Due to the low water solubility of LA, 20% of ethanol in pH 5.5 PBS buffer was then used as an acceptor medium at 32°C. The cumulative amount of LA released from the NE was greater and faster than that from the corresponding NLC and SLN. Our results revealed that up to 62% was released across the NE membrane over the 72-h test period while only 32% and 23% of the LA was released from NLC and SLN, respectively, under the same condition. These results indicated that LA incorporated into both SLN and NLC was likely to remain associated with the nanoparticles. Moreover, no burst release of LA within a few minutes was observed in these systems, indicating that prolonged release of the drugs from the nanoparticles can be achieved. The prolonged release and the lower total release after 72 h of both NLC and SLN can be explained by slower diffusion of LA from solid matrix of the formulations. The presence of solid lipid both in SLN and NLC increase viscosity of nanoparticles, which then slow

Table III. DSC Parameters of LA-Loaded NLC and SLN Formulations Measured After 0, 30, 60, 90, and 120 Days of Storage at 25°C

Formulations	Day of storage	Melting temperature (°C)	Onset temperature (°C)	Enthalpy (J/g)	%Recrystallization
Apifil bulk material	–	68.0	58.7	190.8	100
	0	59.5	29.7	9.8	51.2
	30	60.9	39.1	12.7	66.7
NLC	60	63.0	54.2	14.0	73.5
	90	59.0	43.4	17.6	92.2
	120	58.1	39.8	19.8	103.7
	0	61.8	43.3	14.5	76.0
	30	60.1	45.2	15.7	82.3
SLN	60	62.8	42.4	18.6	97.4
	90	60.6	59.1	21.4	112.2
	120	62.5	42.2	21.0	110.1

NLC nanostructure lipid carriers, *SLN* solid lipid nanoparticles

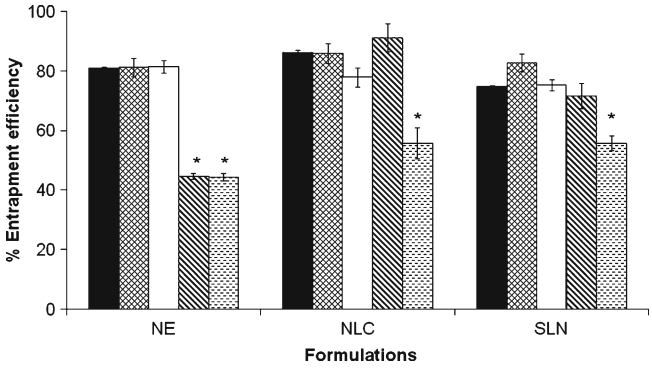

Fig. 4. Percent of entrapment efficiency of LA on LA-loaded NE, NLC, and SLN formulations after 0 (■), 30 (▨), 60 (□), 90 (▧), and 120 (▤) days of storage at 25°C. *The mean difference is significant at the 0.05 level as compared to 0 days of storage

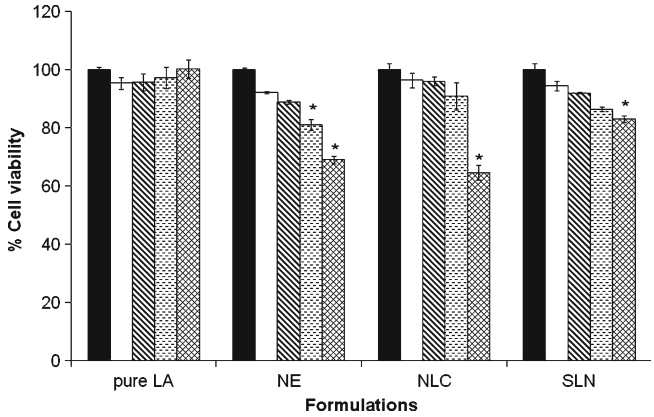

Fig. 6. Cytotoxicity of LA-loaded NE, NLC, and SLN formulations at varying concentration of 0 (■), 0.01 (□), 0.1 (▧), 1 (▤), and 10 (▨) μM of LA in NHF cells after 48 h exposure. *The mean difference is significant at the 0.05 level as compared to control

down the release of LA according to Stokes–Einstein's law (23). It has also been proposed that the incorporation of liquid oil in NLC formulation resulted in lower viscosity of the lipid matrix, following a faster release from NLC when compared to SLN. Moreover, an inhomogeneity of the liquid oil distributed within the inner structure of the lipid matrix would lead to the deposition of liquid oil on the outer shell of NLC after lipid crystallization. This oil layer resulted in faster release of LA from NLC compared to from SLN. It is interesting to note that the release profile was dependent not only on types of formulation type but also on lipid types. Mühlen et al. reported burst release found from tetracaine and etomidate incorporated in Compritol SLN (35). The release data were analyzed with the following Higuchi kinetic equation.

$$Q_t = Kt^{1/2} \tag{3}$$

where Q_t is the percentage of drug released at time t and K is the release rate constant. Regarding the release model of all formulations, it was found that a prolonged release characteristic of LA was well fitted to Higuchi's square root model as has been reported by drug-loaded SLN systems (23,28). This model explains that drug release from a matrix system is directly proportional to the square root of time. Linear fits were obtained indicating that the release profile of LA was diffusion-al-controlled from homogenous and granular matrix systems. The R^2 values from *in vitro* release kinetics were 0.980, 0.993, and 0.982 for NE, NLC, and SLN, respectively. The K values or release rate constant obtained from Higuchi model plot is then proportional to an apparent diffusion coefficient. The K values were 8.563, 3.966, and 3.206 μg cm^{-2} $h^{-1/2}$ for NE, NLC, and SLN, respectively. The K values of both NLC and SLN formulations were closed and much lower than NE, suggesting lower diffusion rate of LA from solid lipid or mixed solid and liquid lipid matrix than liquid matrix alone.

Cytotoxicity Test

To investigate the cytotoxicity of pure LA, NE, NLC, and SLN, the cell viability was determined by MTT assay. The cell viability of each formulation decreased with an increase in concentration of LA from 0 to 10 μM (Fig. 6) whereas percent cell viability of pure LA remained unchanged. A decrease in cell viability of NE, NLC, and SLN was significantly different as compared with control at 1, 10, and 10 μM, respectively. This could be attributed to the presence

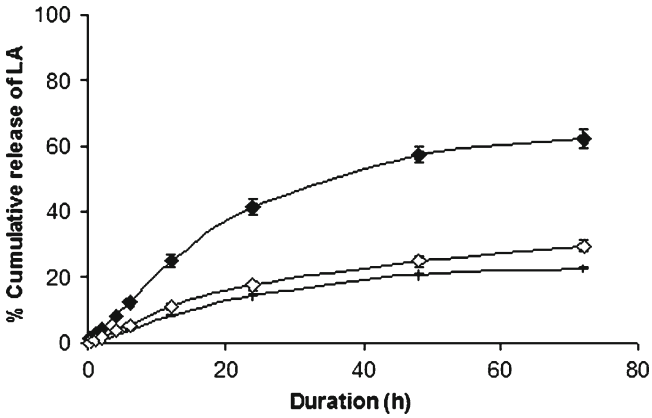

Fig. 5. Release profiles of LA-loaded NE (*filled diamonds*), NLC (*empty diamonds*), and SLN (*plus signs*) formulations

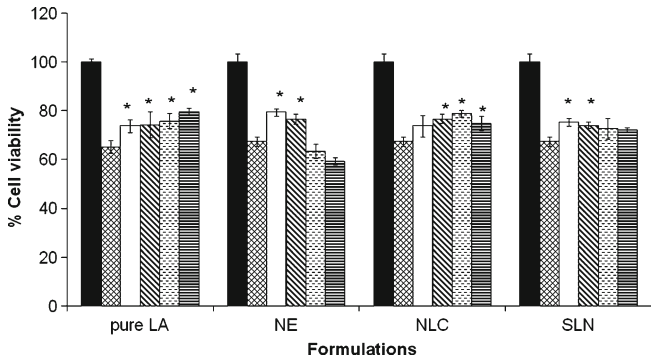

Fig. 7. Antioxidant activity of LA-loaded NE, NLC, and SLN formulations at varying concentration of control (■), hydrogen peroxide (▨), 0.01 (□), 0.1 (▧), 1 (▤), and 10 (▥) μM of LA in NHF cells after 48 h exposure. *The mean difference is significant at the 0.05 level as compared to hydrogen peroxide

of surfactant either free in solution or bound to nanoparticle surfaces, which may then possibly cause cell damaging effect. Calculated surfactant concentrations at varying LA concentrations of 0.01, 0.1, 1, and 10 μM were 0.0006, 0.006, 0.06, and 0.6 μM, respectively. Therefore, the surfactants at concentrations higher than 0.06 μM for NE and 0.6 μM for SLN and NLC were not recommended for further use. However, the percent cell viability of these three formulations remained higher than 80% at LA concentration below 10 μM, indicating their potential use as colloidal carriers *in vivo*. Low cell toxicity was also observed on two SLN systems, which were Dynasan and Compritol in comparison to polymeric polyalkyl cyanoacrylate and polylactic/polyglycolic acid nanoparticles using HL60 cells line (36). Those SLN carriers demonstrated a lower cytotoxicity compared to those polymeric nanoparticles.

Antioxidation Activity

To investigate the antioxidant activity of pure LA and formulations, cell viability after the induction of free radical in human fibroblast using hydrogen peroxide was observed (Fig. 7). The presence of 125 μM of hydrogen peroxide in a cell induced free radicals that may then lead to cell death as seen at 60% cell viability. An increase in the concentration of pure LA, NE, NLC, and SLN has shown to enhance the percent of cell viability at observed concentration from 0.01 to 10 μM. The concentrations that cause significant antioxidation effect were found at 0.01, 0.01, 0.1, and 0.01 μM for pure LA, NE, NLC, and SLN, respectively (p value<0.05). These results indicate that LA incorporated in SLN, NLC, and NE remained effective similarly to pure LA and the hot homogenization process can be successfully employed to prepare aqueous dispersion of water-insoluble active compound. However, it should be noted that, at LA concentration of 1 and 10 μM, a decrease in cell viability was found for NE whereas an insignificant enhancement was obtained for SLN, which could be due to cell toxicity effect at these concentrations of both NE and SLN.

CONCLUSIONS

In this study LA, a poorly water-soluble antioxidation compound was successfully incorporated into lipid nanoparticle formulations (NE, NLC, and SLN). The mean particle size from PCS of all formulations was lower than 200 nm with narrow size distribution. The zeta potentials of NLC and SLN were higher than|−30| mV, suggesting the potential of good physical stability. The less-ordered structure of the lipid matrix of NLC formulations resulted in unchanged entrapment efficiency as well as delayed percent recrystallization index over 90 days. Moreover, a sustained release of LA can be achieved by the presence of solid lipid in SLN or mixed solid lipid and liquid lipid in NLC. All formulations demonstrated antioxidant activity at similar level of 0.01 to 10 μM to pure LA with low cell cytotoxicity. Water-soluble nanoparticles such as NLC and SLN have been proven to be suitable colloidal carriers for the water-insoluble LA and their physicochemical and biological activities suggest their potential use for topical delivery.

ACKNOWLEDGEMENTS

This research was financially supported by the National Nanotechnology Center (NANOTEC), Thailand (research grant number B22 CR0102).

REFERENCES

1. U. Cakatay, A. Telci, R. Kayali, A. Sivas, and T. Akcay. Effect of lipoic acid supplementation on oxidative protein damage in the streptozotocin-diabetic rat. *Res. Exp. Med. (Berl)*. **199**:243–251 (2000).
2. Y. Dincer, A. Telci, R. Kayal, C. Yılmazia, U. Cakatay, and T. Akcay. Effect of a-lipoic acid on lipid peroxidation and antioxidant enzyme activities in diabetic rats. *Clin. Exp. Pharmacol. Physiol*. **29**:281–284 (2002).
3. M. A. Lovell, C. Xie, S. Xiong, and W. R. Markesbery. Protection against amyloid b peptide and iron/hydrogen peroxide toxicity by a-lipoic acid. *J. Alzheimer Dis*. **5**:229–239 (2003).
4. G. H. Marracci, G. P. McKeon, W. E. Marquardt, R. W. Winter, M. K. Riscoe, and D. N. Bourdette. α-Lipoic acid inhibits human T cell migration: implications for multiple sclerosis. *J. Neurosci. Res*. **78**:362–370 (2004).
5. A. R. Smith, S. V. Shenvi, M. Widlansky, J. H. Suh, and T. M. Hagen. Lipoic acid as a potential therapy for chronic diseases associated with oxidative stress. *Curr. Med. Chem*. **11**:1135–1146 (2004).
6. A. Baur, T. Harrer, M. Peukert, G. Jahn, J. R. Kalden, and B. Fleckenstein. Alpha-lipoic acid is an effective inhibitor of human immuno-deficiency virus (HIV-1) replication. *J. Mol. Med*. **69**:722–724 (1991).
7. U. Cakatay. Pro-oxidant actions of a-lipoic acid and dihydrolipoic acid. *Med. Hypotheses*. **66**:110–117 (2006).
8. A. Bliska, and L. Wlodek. Lipoic acid—the drug of the future? Pharmacol. Rep. **57**:570–577 (2005).
9. L. Packer. α-Lipoic acid: a metabolic antioxidant, which regulates NF-κB signal transduction and protects against oxidative injury. *Drug Metab. Rev*. **30**:245–275 (1998).
10. D. Ziegler, and F. A. Gries. Alpha-lipoic acid in the treatment of diabetic peripheral and cardiac autonomic neuropathy. Diabetes. **46**:S62–S66 (1997).
11. S. D. Wollin, and P. J. Jones. Alpha-lipoic acid and cardiovascular disease. J. Nutr. **133**:3327–3330 (2003).
12. J. Fuchs, and R. Milbradt. Antioxidant inhibition of skin inflammation induced by reactive oxidants: Evaluation of the redox couple dihydrolipoate/lipoate. Skin Pharmacol. **7**:278–284 (1994).
13. M. Podda, M. Rallis, M. G. Cuber, L. Packer, and H. Maibachl. Kinetic study of cutaneous and subcutaneous distribution following topical application of [7,8J4C] rac-cx-lipoic acid onto hairless mice. *Biochem. Pharmacol*. **52**:627–633 (1996).
14. H. Beitner. Randomized, placebo-controlled, double blind study on the clinical efficacy of a cream containing 5% α-lipoic acid related to photoageing of facial skin. *Br. J. Dermatol*. **149**:841–849 (2003).
15. R. H. Müller and J. S. Lucks. Medication vehicles made of solid lipid particles (solid lipid nanospheres—SLN). Eur. Patent 0605497 (1996).
16. R. H. Müller, K. Mäder, and S. Gohla. Solid lipid nanoparticles (SLN) for controlled drug delivery—a review of the state of the art. *Eur. J. Pharm. Biopharm*. **50**:161–177 (2000).
17. R. H. Müller, and C. M. Keck. Challenges and solutions for the delivery of biotech drugs—a review of drug nanocrystal technology and lipid nanoparticles. *J. Biotech*. **113**:151–170 (2004).
18. E. Ugazio, R. Cavalli, and M. R. Gasco. Incorporation of cyclosporin A in solid lipid nanoparticles (SLN). *Int. J. Pharm*. **241**:341–344 (2002).
19. S. A. Wissing, and R. H. Müller. Cosmetic applications for solid lipid nanoparticles (SLN). *Int. J. Pharm*. **254**:65–68 (2003).
20. S. A. Wissing, and R. H. Müller. The influence of solid lipid nanoparticles on skin hydration and viscoelasticity—*in vivo* study. *Int. J. Pharm*. **56**:67–72 (2003).

21. K. Jores, W. Mehnert, M. Drechsler, H. Bunjes, C. Johann, and K. Mäder. Investigations on the structure of solid lipid nanoparticles (SLNs) and oil-loaded solid lipid nanoparticles by photon correlation spectroscopy, field-flow fractionation and transmission electron microscopy. *J. Controlled Release*. **95**:217–227 (2004).
22. W. Mehnert, and K. Mäder. Solid lipid nanoparticles: production, characterization and applications. *Adv. Drug. Deliv. Rev*. **47**:165–196 (2001).
23. V. Teeranachaideekul, E. B. Souto, V. B. Junyaprasert, and R. H. Müller. Cetyl palmitate-based NLC for topical delivery of coenzyme Q10—development, physicochemical characterization and *in vitro* release studies. *Eur. J. Pharm. Biopharm*. **67**:141–148 (2007).
24. C. Freitas, and R. H. Müller. Correlation between long-term stability of solid lipid nanoparticles (SLN™) and crystallinity of the lipid phase. *Eur. J. Pharm. Sci*. **47**:125–132 (1999).
25. A. Ernst, A. Stolzing, G. Sandig, and T. Grune. Antioxidants effectively prevent oxidation-induced protein damage in OLN 93 cells. *Arch. Biochem. Biophys*. **421**:54–60 (2004).
26. M. A. Schubert, and C. C. Müller-Goymann. Characterisation of surface-modified solid lipid nanoparticles (SLN): influence of lecithin and nonionic emulsifier. *Eur. J. Pharm. Biopharm*. **61**:77–86 (2005).
27. A. Saupe, K. C. Gordon, and T. Rades. Structural investigations on nanoemulsions, solid lipid nanoparticles and nanostructured lipid carriers by cryo-field emission scanning electron microscopy and Raman spectroscopy. *Int. J. Pharm*. **314**:56–62 (2006).
28. W. Tiyaboonchai, W. Tungpradit, and P. Plianbangchang. Formulation and characterization of curcuminoids loaded solid lipid nanoparticles. *Int. J. Pharm.* **337**:299–306 (2007).
29. H. Bunjes, K. Westesen, and M. H. J. Koch. Crystallization tendency and polymorphic transitions in triglyceride nanoparticles. *Int. J. Pharm*. **129**:159–173 (1996).
30. A. Saupe, S. A. Wissing, A. Lenk, C. Schmidt, and R. H. Müller. Solid lipid nanoparticles (SLN) and nanostructured lipid carriers (NLC)—structural investigations on two different carrier systems. *Biomedical Mater*. **15**:393–402 (2005).
31. V. Jenning, A. F. Thünemann, and S. H. Gohla. Characterisation of a novel solid lipid nanoparticle carrier system based on binary mixtures of liquid and solid lipids. *Int. J. Pharm*. **199**:167–177 (2000).
32. V. Jenning, and S. Gohla. Comparison of wax and glyceride solid lipid nanoparticles (SLN®). *Int. J. Pharm*. **196**:219–222 (2000).
33. V. Jenning, and S. H. Gohla. Encapsulation of retinoids in solid lipid nanoparticles (SLN). *J. Microencapsul*. **18**:149–158 (2001).
34. E. B. Souto, S. A. Wissing, C. M. Barbosa, and R. H. Müller. Development of a controlled release formulation based on SLN and NLC for topical clotrimazole delivery. *Int. J. Pharm*. **278**:71–77 (2004).
35. A. Z. Mühlen, C. Schwarz, and W. Mehnert. Solid lipid nanoparticles (SLN) for controlled drug delivery—drug release and release mechanism. *Eur. J. Pharm. Biopharm*. **45**:149–155 (1998).
36. R. H. Müller, D. Rühl, S. Runge, K. Schulze-Forster, and W. Mehnert. Cytotoxicity of solid lipid nanoparticles as a function of the lipid matrix and the surfactant. *Pharm. Res*. **14**:458–462 (1997).